CURVED BOUNDARY TREATMENT OF THE LATTICE BOLTZMANN METHOD FOR SLIP FLOW SIMULATIONS

Namgyun Jeong*
Division for Research Reactor System Design, Korea Atomic Energy Research Institute

Slip flow 해석을 위한 격자볼츠만 방법의 곡면처리기법

정 남 균*
한국원자력연구원 연구로 계통설계부

The lattice Boltzmann (LB) method has been used to simulate rarefied gas flows in a micro-system as an alternative tool. However, previous results were mainly focused on a simple geometry with flat walls because the LB method is modeled on uniform Cartesian lattices. When previous boundary conditions for the microflows are applied to curved walls, the use of them requires approximation of the curved boundary by a series of stair steps, and introduces additional errors. For macroflows, no-slip curved wall boundary treatments have been developed remarkably in order to overcome these limits. However, the investigations for the slip curved wall boundary have rarely been performed for microflows. In this work, a curved boundary treatment of the LB method for a slip flow has been introduced. The results of the LB method for 2D microchannel and 3D microtube flows are in excellent agreement with the analytical solutions.

Key Words : Curved boundary condition; Lattice Boltzmann method; Microflow; Rarefied gas flow

1. Introduction

The lattice Boltzmann (LB) method has been used widely to simulate fluid flows as an alternative tool. Recently, the LB method has been used to simulate rarefied gas flows in microsystems successfully. In a micron-sized system, the molecular mean free path of fluid molecules may be about the same order of magnitude as the typical geometric dimension of the device. The effect of the mean free path can be characterized by the Knudsen number *Kn*, which is the ratio of the mean free path to the characteristic length. For *Kn* greater than 0.01, the slip at the solid wall becomes an important flow feature.

Because the boundary treatments influence the accuracy and stability, developing accurate and efficient boundary condition for the LB simulations has become one of the most interesting subjects in many engineering and scientific applications. However, while the curved boundary treatments of the LB simulations for macroflows have been developed remarkably and are popularly used to fulfill no-slip on the wall[1-5], the investigations for the microflows have been performed much less than those for the macroflows. Szalmás[6] presented a slip-flow boundary condition for straight walls placed at an arbitrary position combining an interpolation method and a simple slip boundary condition. Watari[7] studied a rotational slip flow in coaxial cylinders by using multi-speed finite-difference LB models and adopting the cylindrical coordinate system. His FDLBM model with 24 directions showed accurate results even at large *Kn*. However, finding an arbitrary curved boundary treatment of LB method for a slip flow is still a challenging problem.

The remainder of this paper is organized as follows. Sec. 2 briefly reviews the LB method for the slip flow simulations. In Sec. 3, the description about a curved

Received: July 15, 2014, Revised: August 28, 2014, Accepted: August 28, 2014.
* E-mail: jng@kaeri.re.kr
DOI http://dx.doi.org/10.6112/kscfe.2014.19.3.077

boundary treatment for the slip flow is presented. Sec. 4 is devoted to the comparison of the results of the LB method with analytical solutions for 2D microchannel flows, which have an arbitrarily positioned wall between the fluid and wall nodes, and 3D microtube flows. The conclusion is given in Sec. 5.

2. Lattice Boltzmann Method

For a flow without an external force, the following lattice Boltzmann equation is available.

$$f_\alpha(\vec{x}+\vec{e_\alpha}\delta t, t+\delta t)-f_\alpha(\vec{x},t) = -\frac{1}{\tau+0.5}\left(f_\alpha-f_\alpha^{eq}\right)|_{(\vec{x},t)} \quad (1)$$

where f_α is the particle distribution function; $\vec{e_\alpha}$ is the microscopic velocity; and τ is the relaxation time. The equilibrium distribution function is given by

$$f_\alpha^{eq} = t_\alpha \rho\left[1+\frac{\vec{e_\alpha}\cdot\vec{u}}{c_s^2}+\frac{\left(\vec{e_\alpha}\cdot\vec{u}\right)^2}{2c_s^4}-\frac{u^2}{2c_s^2}\right], \quad (2)$$

where t_α is a weighting factor; ρ is the density of the system; $\vec{u}$ is the macroscopic velocity; and c_s is the speed of sound. The square lattice (D2Q9) and 3D 19-velocity (D3Q19) LBM models are used for the 2D and 3D simulations, respectively[8]. The macroscopic density, kinematic viscosity, and momentum are recovered by

$$\rho=\sum_\alpha f_\alpha\,;\ \nu=\frac{\tau}{3}\frac{\delta x^2}{\delta t};\ \text{and}\ \rho\vec{u}=\sum_\alpha \vec{e_\alpha} f_\alpha. \quad (3)$$

For rarefied gas simulations with the LB method, the relaxation time, τ, needs to be related to *Kn*. From the kinetic theory, it can be assumed that the gas molecules represented by the particle distribution functions travel the distance of the lattice mean-free path l with the mean thermal speed defined as $\bar{c}=\sqrt{8kT/\pi m}$, while relaxing to their equilibrium state in the relaxation time λ.. The mean thermal speed $\bar{c}$ can be represented with the lattice velocity c which depends on the lattice model[8], e.g., $c=\sqrt{3kT/m}$ for D2Q9 and D3Q19 models.

$$\bar{c}=\sqrt{\frac{8}{3\pi}}\,c=\sqrt{\frac{8}{3\pi}}\,\frac{\delta x}{\delta t} \quad (4)$$

Therefore, the Knudsen number can be expressed as follows[9]:

$$Kn=\frac{l}{H}=\frac{\lambda\bar{c}}{H}=\sqrt{\frac{8}{3\pi}}\,\frac{\lambda}{\delta t}\frac{\delta x}{H}=\sqrt{\frac{8}{3\pi}}\,\tau\frac{\delta x}{H} \quad (5)$$

where H is the characteristic length, which is either the channel height or the radius of a tube.

3. Curved boundary treatment for the slip flow

For a slip boundary condition of the LB method, Lee and Lin[10] used the equilibrium wall boundary condition with the assumption that reflection of molecules impinging on the wall is diffuse so that molecules reach equilibrium at the wall during the relaxation time. Therefore, the equilibrium distribution function of Eq. (2) with the density and velocity at the wall is used for the particle distribution function at the boundary node. When it is applied to the rarefied gas flow simulation, the results are in excellent agreement with the analytic solutions. However, wall surfaces are always located halfway between two grid points for the second-order accuracy. Therefore, for a curved geometry, Lee and Lin's boundary condition requires the boundary to be approximated by a series of stair steps, and a curved boundary treatment needs to be proposed to overcome that shortcoming.

To use the concept of the equilibrium wall boundary for a curved boundary, it is necessary to consider the above sentence, "wall surfaces are always located halfway between two grid points", from a different point of view, i.e., we can put two imaginary grid points half lattice spacing apart from the wall surface in opposite directions. One point may be located in the fluid side, and the other in the wall side. Among them, we only need to know the information of the particle distribution function at the grid point in the wall side to obtain the particle distribution function at the real boundary node, and it can be easily calculated from Eq. (2) fortunately. With this intuition, deriving a curved boundary treatment for a slip flow can be started by putting an imaginary wall node (r_W) at the position of $0.5\delta x$ apart from the wall surface (see Fig. 1), and assigning the equilibrium distribution function to the particle distribution function at r_W, i.e., $f_\alpha(r_W)=f_\alpha^{eq}(\rho_W,u_W)$. u_W is the surface velocity, and ρ_W is the density at r_W. As an approximation of ρ_W, the density at the location of boundary node (r_B) can be used. Therefore, the particle distribution function at r_W

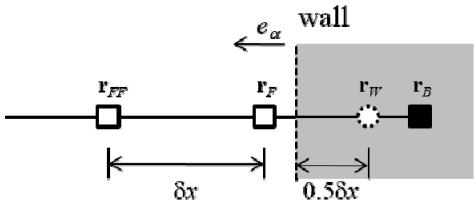

Fig. 1 1D lattice distribution and wall surface: r_F is the outer most fluid node; r_W is the imaginary wall node which can be located half lattice spacing apart from the wall surface; and r_B is the boundary node

can be approximated as $f_\alpha(r_W) \approx f_\alpha^{eq}(\rho_B, u_W)$.

The particle distribution function of the boundary, $f_\alpha(r_B)$, can then be obtained by interpolation/ extrapolation using the information in the surrounding nodes, $f_\alpha(r_F)$, $f_\alpha(r_{FF})$, and $f_\alpha(r_W)$ as follows:

$$f_\alpha(r_B) = Af_\alpha(r_W) + Bf_\alpha(r_F) + Cf_\alpha(r_{FF}) \tag{6}$$

where A, B and C are constants related to the interpolation/ extrapolation method. When linear interpolation/ extrapolation is applied,

$$\begin{aligned} A &= 1/(\triangle + 0.5) \\ B &= (\triangle - 0.5)/(\triangle + 0.5) \\ C &= 0 \end{aligned} \tag{7}$$

where Δ is the fraction of the intersected link in the fluid region, which can be defined as follows:

$$\triangle \equiv \frac{|r_F - r_W - 0.5\delta x|}{|r_F - r_B|} \tag{8}$$

4. Numerical simulation

4.1 Microchannel flow

The present curved boundary condition for the slip flow is applied for the simulation of a channel flow. The 2D channel, which has straight walls placed at an arbitrary position between the fluid node and wall node, is considered.

The analytic solution of fully developed velocity profile for the isothermal flow between two parallel plates can be deduced from the Navier-Stokes equation using the slip boundary condition. When the second-order slip model and fully diffused walls are considered, the slip velocities are

$$u_s = \alpha l \frac{\partial u}{\partial n}|_{wall} - \beta l^2 \frac{\partial^2 u}{\partial n^2}|_{wall} \text{ for the lower wall,} \tag{9}$$

and

$$u_s = -\alpha l \frac{\partial u}{\partial n}|_{wall} - \beta l^2 \frac{\partial^2 u}{\partial n^2}|_{wall} \text{ for the upper wall,} \tag{10}$$

where u_s and n are the slip velocity and wall normal coordinate. For a flat wall, Hadjiconstantinou[11] has proposed slip coefficients α=1.11 and β=0.61 from the accurate numerical solutions of the Boltzmann equation for a hard sphere gas.

Under the assumption of a long channel, the following analytical solutions can be deduced with Eq. (9) and Eq. (10).

$$u(y) = -\frac{H^2}{2\mu}\frac{dP}{dx}\left[-\left(\frac{y^2}{H^2}\right) + \left(\frac{y}{H}\right) + 1.11Kn + 1.22Kn^2\right] \tag{11}$$

$$1 - \tilde{P}^2 + 13.32Kn_o(1-\tilde{P}) - 14.64Kn_o^2 \times \ln\tilde{P} = \xi(1-\tilde{x}) \tag{12}$$

where $\tilde{P} = P/P_o$, normalized pressure with the outlet pressure; $\tilde{x} = x/L$, the coordinate normalized with the channel length; and ξ a constant such that $\tilde{P}(0) = P_i/P_o$.

To compare the results using presented boundary condition with those of previous curved boundary treatments[2,3], which have been used for macroflows, the gas flows in a 2D long microchannel, whose length and height are L and H, are simulated. The unknown particle distribution functions at the inlet and outlet are calculated by second-order extrapolation of those adjacent to the boundary nodes. Following the extrapolation, the calculated densities at the inlet and outlet are rescaled to make the average density across the inlet and outlet boundary nodes the same as the prescribed density.

Fig. 2 shows the results for Kn_o=0.05 compared with the analytical solutions of Eq. (11) and Eq. (12). The grid size for H is restricted to $30\delta x$, and L/H=80 is used in order to investigate the compressibility and rarefaction effects on a sufficiently long micro-channel flow. The channel height, H, can be presented as $(N_H - 3 + 2\triangle)\delta x$, where N_H is the number of lattice sites, and Δ is fixed to 1 because the previous boundary treatment becomes simpler and gives stable results when Δ is greater than 0.75[2,3]. For all calculations, P_i/P_o is set to 2.0. The nonlinearity of pressure, i.e. deviation of the pressure from the linear pressure distribution, (P - P_{incomp}), is normalized by the outlet pressure, P_o, and the

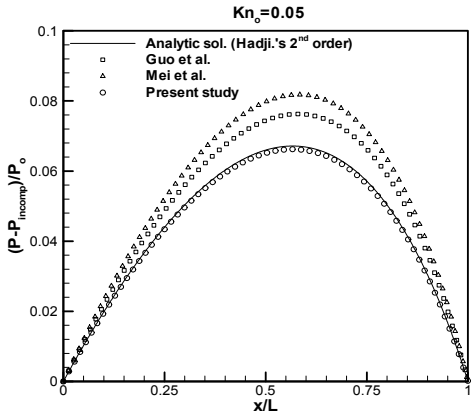

(a) Pressure

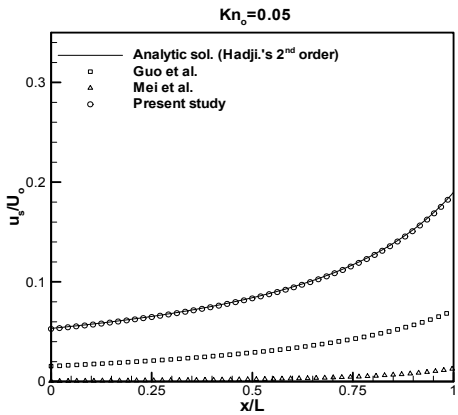

(b) Slip velocity

Fig. 2 Nonlinearity of pressure and slip velocity distributions for Kn_o=0.05 at P_i/P_o=2.0, H=30δx, and L/H=80

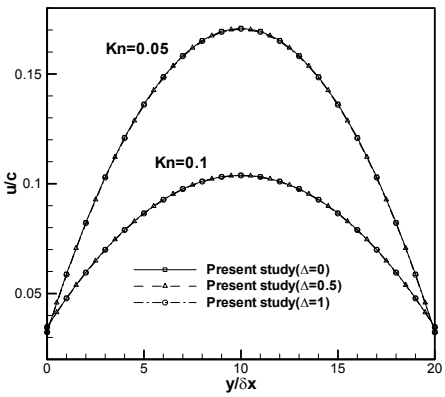

Fig. 3 Velocity profiles of microchannel flows for the cases of Δ=0, 0.5, and 1

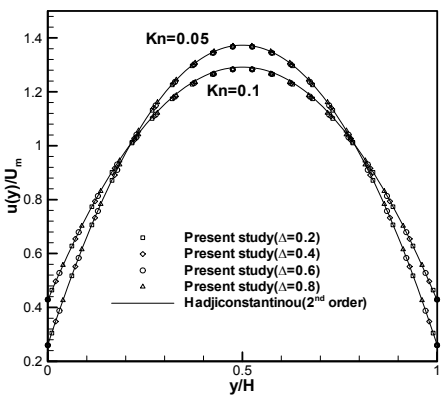

Fig. 4 Comparison of non-dimensional velocity distribution in a microchannel with the analytical solution

stream direction, x, is normalized by the channel length. Slip velocities are normalized by the outlet centerline velocity U_o. For the present boundary treatment, the results are in excellent agreement with the analytical solutions, while the results of curved boundary treatments for macroflow deviate much from them.

In order to investigate the effect of variation of Δ on the results, simulations of the gas flow in an infinitely long microchannel are carried out. To mimic the flow, a periodic microchannel flow driven by a constant external pressure gradient is considered. In the presence of a body force, the LB equation must be modified to account for the force by adding an additional term to Eq. (1) as follows[12].

$$f_\alpha(\vec{x}+\vec{e_\alpha}\delta t, t+\delta t) - f_\alpha(\vec{x},t) = -\frac{1}{\tau+0.5}\left(f_\alpha - f_\alpha^{eq}\right)|_{(\vec{x},t)} + \delta t F_\alpha \quad (13)$$

where $F_\alpha = \left(1-\frac{1}{2\tau+1}\right) t_\alpha \left[\frac{\vec{e_\alpha}-\vec{u}}{c_s^2} + \frac{(\vec{e_\alpha}\cdot\vec{u})}{c_s^4}\vec{e_\alpha}\right]\cdot\vec{F}$.

For the external pressure gradient, $F_x = -\partial P/\partial x$ is applied.

Fig. 3 shows the velocity profiles along the channel height. The channel height, H, and external pressure gradient, F_x, are 20δx and 0.001. The results of Δ=0, 0.5, 1 should be in exact agreement with one another because H and F_x are fixed. For the cases of Kn=0.05 and 0.1, the profiles are seen to be independent on Δ, which shows the boundary condition is functioning properly. In Fig. 4, the results of the analytical solution are compared with those of present study. The values of Δ from 0.2 to 0.8 in increments of 0.2 are used. The velocity profiles are non-dimensionalized by the mean velocity U_m, which can be presented analytically as

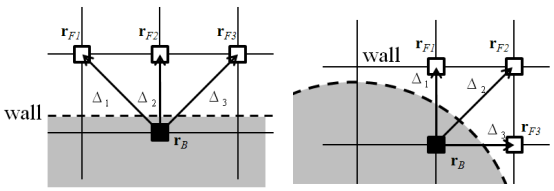

(a) Flat wall (b) Curved wall

Fig. 5 Lattice distribution with arbitrary Δ near a flat wall and a curved wall

$$U_m = -\frac{H^2}{2\mu}\frac{dP}{dx}\left[\frac{1}{6}+1.11Kn+1.22Kn^2\right]. \quad (14)$$

The results of the LB method are in excellent agreement with the analytical solution, and the symbols representing the cases of Δ=0.2~0.8 lie on the same curves.

4.2 Microtube flow

Poiseuille flow in a microtube, which has circular cross section, is considered for 3D simulation with a curved geometry. For the channel flow, Δ is fixed as a certain value. In the tube flow, however, Δ varies along the wall boundary, and sometimes it may has different value according to the direction of discrete velocity even on the same wall node (see Fig. 5).

Therefore, a microtube flow is a more serious problem in achieving accurate results using the LB method under uniform Cartesian lattices.

The velocity profile for the microtube is

$$u(r) = -\frac{R^2}{4\mu}\frac{dP}{dx}\left[1-\left(\frac{r}{R}\right)^2\right]+C, \quad (15)$$

where dP/dx is the pressure gradient in the axial direction, R is a radius of a tube, and C is a constant, which is determined from the slip flow boundary condition at the wall. In contrast to the case of channel flow, there is a lack of precise experimental data and appropriate slip model in the microtube flow. Weng et al.[13] presented following slip model for the microtube flow,

$$u_s = -al\left(\frac{2}{\sqrt{\pi}}\frac{1}{Kn}\right)^d \frac{\partial u}{\partial r}\Big|_{wall} - \frac{b}{2}\left(\frac{2}{\sqrt{\pi}}\frac{1}{Kn}\right)^c R^2\frac{\partial^2 u}{\partial r^2}\Big|_{wall} \quad (16)$$

where a, b, c and d are coefficients obtained by comparing the solutions of linearized Boltzmann

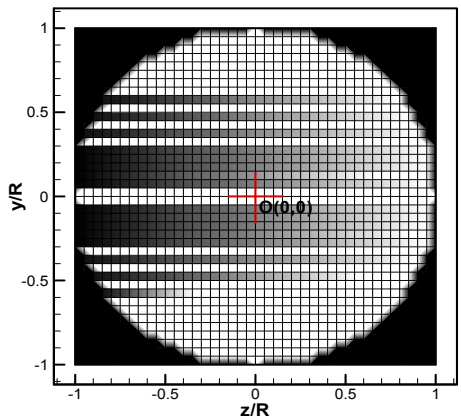

Fig. 6 Calculation domain in a cross section of a tube. The fluid and wall regions are distinguished by white and black colors, respectively. The initial origin is $(y,z)=(0,0)$ and marked by a cross

equation[14]: a=0.49; b=1.28; c=-1.0669; and d=-0.003. The Knudsen number is defined as $Kn=l/R$ for the tube flow.

When the slip model is considered, the velocity distribution can be obtained from Eq. (15) and Eq. (16), i.e.,

$$u(r) = -\frac{R^2}{4\mu}\frac{dP}{dx}\left[1-\left(\frac{r}{R}\right)^2+\frac{4a}{\sqrt{\pi}}\left(\frac{2}{\sqrt{\pi}}\frac{1}{Kn}\right)^{d-1}+b\left(\frac{2}{\sqrt{\pi}}\frac{1}{Kn}\right)^2\right]. \quad (17)$$

Fig. 6 shows the calculation domain in a cross section of a tube indicating the fluid and wall regions with white and black colors, respectively. The initial origin is located at the coordinate of $(y,z)=(0,0)$.

The results for $R=20\delta x$ and Kn=0.1 are shown in Fig. 7. The origin is varied from $(y,z)=(0,0)$ to $(y,z)=(0,0.5\delta x)$, while the tube radius is kept as $R=20\delta x$. The velocity distribution is normalized by the mean velocity U_m as follows:

$$\frac{u(r)}{U_m} = \frac{1-\left(\frac{r}{R}\right)^2+\frac{4a}{\sqrt{\pi}}\left(\frac{2}{\sqrt{\pi}}\frac{1}{Kn}\right)^{d-1}+b\left(\frac{2}{\sqrt{\pi}}\frac{1}{Kn}\right)^c}{\frac{1}{2}+\frac{4a}{\sqrt{\pi}}\left(\frac{2}{\sqrt{\pi}}\frac{1}{Kn}\right)^{d-1}+b\left(\frac{2}{\sqrt{\pi}}\frac{1}{Kn}\right)^c} \quad (18)$$

In principle, moving the origin must not influence the velocity profile, and it does not seem to affect the results when the present boundary condition is used. However, noticeable deviation can be captured in the figure for the

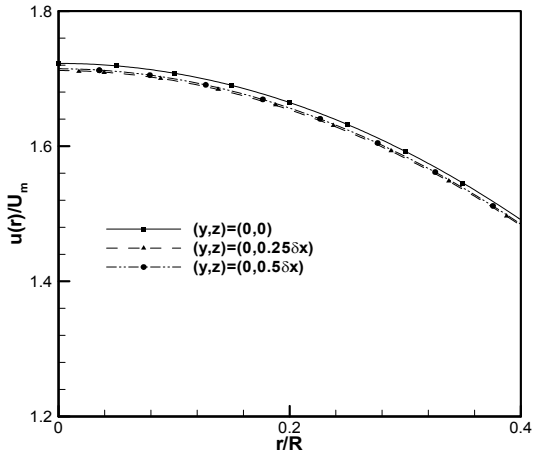

(a) Lee and Lin's boundary condition

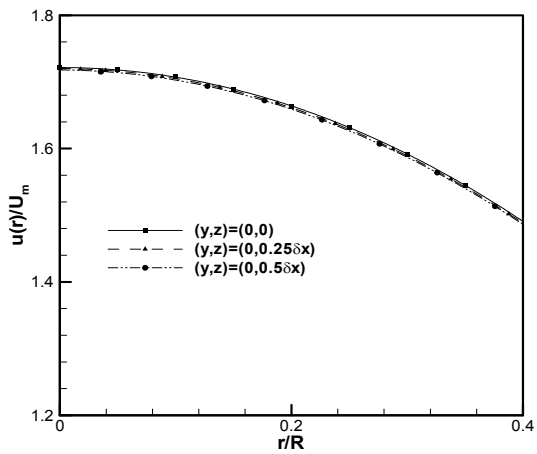

(b) Present curved boundary condition

Fig. 7 Non-dimensional velocity profiles for microtube flows with various origin, (y,z)=(0,0), (0,0.25δx), and (0,0.5δx): Calculation results using Lee and Lin's boundary and present curved boundary condition

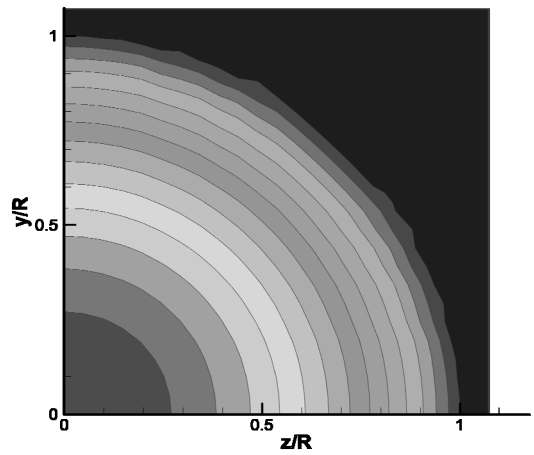

(a) Lee and Lin's boundary condition

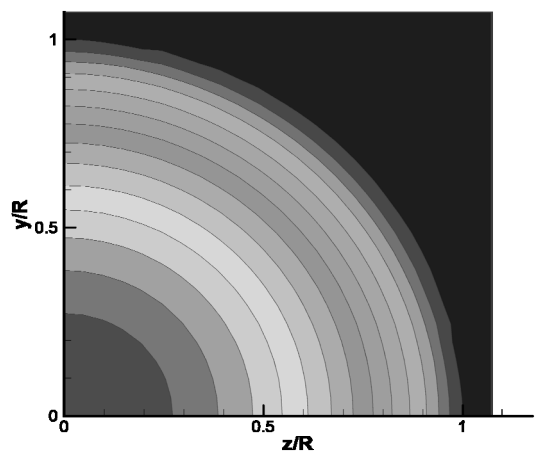

(b) Present curved boundary condition

Fig. 8 Velocity contours in the cross section of a microtube: Calculation results using Lee and Lin's boundary, and present curved boundary condition

case of Lee and Lin's boundary condition. Fig. 8 shows the velocity contours in a cross section of the tube. A closer look of the velocity contours reveals that Lee and Lin's boundary condition creates some wiggled area near the wall. When adapted the present boundary condition, however, the degree of wiggling is apparently decreased.

In Fig. 9, the non-dimensional velocity distribution is compared with the results of the analytical solution of Eq. (16) and the linearized Boltzmann equation[15]. It shows that the solution of LB method with present curved boundary condition is in excellent agreement with the analytic solution. When it is compared with the result of the linearized Boltzmann equation, the LB solution shows excellent agreement except only near the wall. The discrepancy between the results at the wall comes from the Knudsen layer effect. The Knudsen layer is the kinetic boundary layer as a gas flows over a solid wall, and it becomes significant to capture the gas motion for a rarefied or micro gas flow. It is known that the mean free path of gas molecules in the Knudsen layer is smaller than the bulk mean free path. This problem cannot be solved by changing boundary condition.

To consider the Knudsen layer effect, the local relaxation time should be determined by introducing the local mean free path. For a case of flat plate wall, several researchers have obtained good results by adopting the

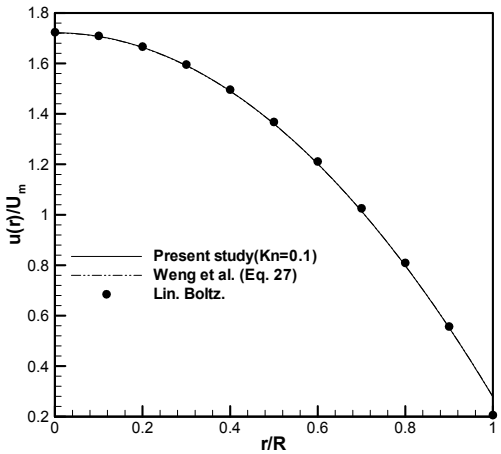

Fig. 9 Comparison of non-dimensional velocity distribution in a microtube with the analytical solution and the simulation results of the linearized Boltzmann equation

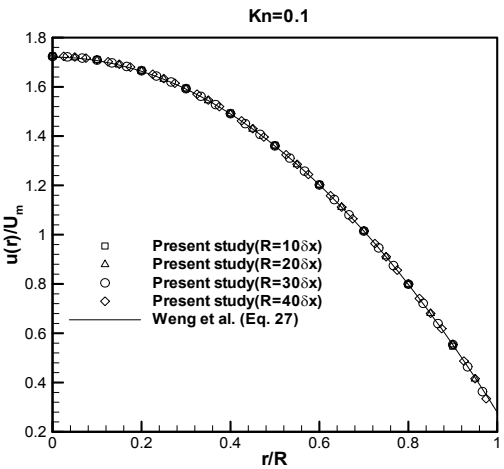

Fig. 10 The effect of grid size across the tube radius on the velocity distribution for Kn=0.1

local relaxation time, but for a case of microtube, it still remains as a challenging topic. The grid sensitivity test is shown in Fig. 10. For the calculations, four refined grids (R=10δx, 20δx, 30δx, and 40δx) and Kn=0.1 are used. It is seen that the accuracy of the solutions is essentially independent of grid size.

Finally, Fig. 11 compares the velocity profiles from the present LB method with the analytical solutions of Weng et al.[13] for various Kn. The tube radius is fixed as R=20δx ,and Kn=0.025, 0.05, and 0.1 are considered. For all calculations, the symbols representing the LB results are exactly located on the lines of analytical solutions.

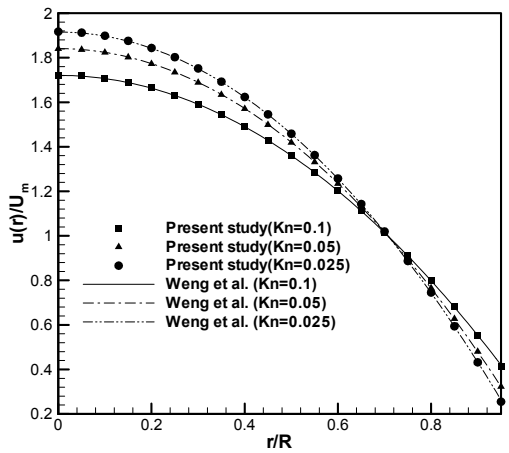

Fig. 11 Comparison of non-dimensional velocity distribution in a microtube with the analytical solution for various Kn

5. Conclusion

In this work, a curved boundary treatment for the slip flow in the LB method has been introduced based on the idea that a virtual wall node can be located half lattice spacing apart from the wall surface. For a comparison of the results of the LB method with analytical solutions, 2D microchannel flows, which have an arbitrarily positioned wall between the fluid and wall nodes, and 3D microtube, which has circular cross section, flows are considered. It is found that the proposed boundary treatment can be applied successfully for simulations with curved geometry. The simulation results using the treatment are essentially independent of the grid size. The application method of the treatment is very simple. By using this treatment, therefore, it is expected to fulfill the slip flow simulation with complex and arbitrary geometries with ease.

Reference

[1] 1998, Filippova, O. and Hänel, D., "Grid Refinement for Lattice-BGK Models," *J. Comput. Phys.*, Vol.147, pp.219-228.

[2] 1999, Mei, R., Luo, L.S. and Shyy, W., "An Accurate Curved Boundary Treatment in the Lattice Boltzmann Method," *J. Comput. Phys.*, Vol.155, pp.307-330.

[3] 2002, Guo, Z., Zheng, C. and Shi, B., "An extrapolation method for boundary conditions in lattice Boltzmann method," *Phys. Fluids*, Vol.14, pp.2007-2010.

[4] 2004, Feng, Z.G. and Michaelides, E.E., "The immersed boundary-lattice Boltzmann method for solving fluid-particle interaction problems," *J. Comput. Phys.*, Vol.195, pp.602-628.
[5] 2007, Shu, C., Liu, N. and Chew, Y.T., "A novel immersed boundary velocity correction-lattice Boltzmann method and its application to simulate flow past a circular cylinder," *J. Comput. Phys.*, Vol.226, pp.1607-1622.
[6] 2006, Szalmás, L., "Slip-flow boundary condition for straight walls in the lattice Boltzmann model," *Phys. Rev. E*, Vol.73, p.066710.
[7] 2011, Watari, M., "Rotational Slip Flow in Coaxial Cylinders by the Finite-Difference Lattice Boltzmann Methods," *Commun. Comput. Phys.*, Vol.9, pp.1293-2314.
[8] 1992, Qian, Y.H., d'Humieres, D. and Lallenmand, P., "Lattice BGK models for Navier-Stokes equation," *Europhys. Lett.*, Vol.17, pp.479-484.
[9] 2005, Zhang, Y.H., Qin, R., Sun, Y.H., Barber, R.W. and Emerson, D.R., "Gas Flow in Microchannels - A Lattice Boltzmann Method Approach," *J. Stat. Phys.*, Vol.121, pp.257-267.
[10] 2005, Lee T. and Lin, C.L., "Rarefaction and compressibility effects of the lattice Boltzmann equation method in a gas microchannel," *Phys. Rev. E*, Vol.71, p.046706.
[11] 2003, Hadjiconstantinou, N.G., "Comment on Cercignani's second-order slip coefficient," *Phys. Fluids*, Vol.15, pp.2352-2354.
[12] 2002, Guo, Z., Zheng, C. and Shi, B., "Discrete lattice effects on the forcing term in the lattice Boltzmann method," *Phys. Rev. E*, Vol.65, p.046308.
[13] 1999, Weng, C., Li, W.L. and Hwang, C.C., "Gaseous flow in microtube at arbitrary Knudsen numbers," *Nanotechnology*, Vol.10, pp.373-379.
[14] 1969, Loyalka, S.K., "Thermal transpiration in a cylindrical tube," *Phys. Fluids*, Vol.12, pp.2301-2305.
[15] 1990, Loyalka S.K. and Hamoodi, S.A., "Poiseuille flow of a rarefied gas in a cylindrical tybe: Solution of linearized Boltzmann equation," *Phys. Fluids A*, Vol.2-11, pp.2061-2065.